A Quantum Convolutional Neural Network for Image Classification

Yanxuan Lü[1], Qing Gao[1,2], Jinhu Lü[1,2], Maciej Ogorzałek[3], Jin Zheng[1]

1. School of Automation Science and Electrical Engineering, Beihang University, Beijing 100191, P. R. China

2. Beijing Advanced Innovation Center for Big Data and Brain Computing, Beihang University, Beijing 100191, P. R. China

3. Department of Information Technologies, Jagiellonian University, Kraków 30-348, Poland

E-mail: lvyanxuan@buaa.edu.cn; gaoqing@buaa.edu.cn; jhlu@iss.ac.cn; maciej.ogorzalek@uj.edu.pl; zhengjin03@buaa.edu.cn

arXiv:2107.03630v1 [quant-ph] 8 Jul 2021

Abstract: Artificial neural networks have achieved great success in many fields ranging from image recognition to video understanding. However, its high requirements for computing and memory resources have limited further development on processing big data with high dimensions. In recent years, advances in quantum computing show that building neural networks on quantum processors is a potential solution to this problem. In this paper, we propose a novel neural network model named *Quantum Convolutional Neural Network* (QCNN), aiming at utilizing the computing power of quantum systems to accelerate classical machine learning tasks. The designed QCNN is based on implementable quantum circuits and has a similar structure as classical convolutional neural networks. Numerical simulation results on the MNIST dataset demonstrate the effectiveness of our model.

Key Words: Quantum Computing; Machine Learning; Neural Network; Quantum Convolutional Neural Network

1 Introduction

Artificial neural network (ANN) has been one of the most critical and widely used models in the field of classical machine learning for its powerful ability to learn complex nonlinear mappings. An important kind of ANN is the convolutional neural network (CNN), which was primarily designed for image recognition tasks [1, 2]. Two special layers of CNN, namely convolutional layers and pooling layers, are stacked to form a hierarchical architecture. This particular structure brings CNN strong abilities to extract structured information using a relatively small amount of parameters. Variants of CNNs have achieved state-of-the-art results on various image-based tasks, and related reviews can be found in [3].

As a research frontier in the field of quantum artificial intelligence, quantum machine learning (QML) [4–8], the interdisciplinary field of quantum computing and machine learning, has gained increasing attention. QML principally implements machine learning algorithms on quantum hardware such as quantum annealers and quantum circuits. Based on quantum properties such as superposition, entanglement, and quantum parallelism, QML has the potential to solve the problems involving big data and slow training process in current classical machine learning with efficiency better than its classical counterpart. In recent years, along with the significant advances of quantum computation techniques [9, 10], the so-called noisy intermediate-scale quantum (NISQ) [11] processors have become one of the most useful hardware platform for implementation of various QML algorithms due to their relatively stable computing capabilities and robustness against decoherence. In particular, artificial neural network models that can be implemented on quantum circuits have been proposed and are named quantum neural networks (QNNs) in the literature [12–14]. The existing approaches can be roughly divided into two classes: one imitates the linear and nonlinear operations of ANNs; the other one utilizes parameterized quantum circuits as trainable neurons and imitates the hierarchy of ANNs. Moreover, many proof-of-principle experiments using real quantum computers have been carried out.

Among various QNNs, the quantum convolutional neural networks (QCNNs) imitating the structure or operations of classical CNNs were proposed. Cong *et al.* [15] designed a quantum circuit model with a similar hierarchy to classical CNNs, which dealt with quantum data and could be used to recognize phases of quantum states and to devise a quantum error correction scheme. The convolutional and pooling layers were approximated by quantum gates with adjustable parameters. Ref. [16] proposed a new quanvolutional (short for quantum convolutional) filter, in which a random quantum circuit was deployed to transform input data locally. Quanvolutional filters were embedded into classical CNNs, forming a quantum-classical hybrid structure. In addition, a more complex QCNN design was presented in the most recent work [17], where delicate quantum circuits were employed to accomplish quantum inner product computations and approximate nonlinear mappings of activation functions.

In this paper, motivated by the network structure in [15] and recent research about the expressive power [18] as well as quantum advantages on low-depth quantum circuits [19], we propose a novel quantum convolutional neural network model based on parameterized quantum circuits for image classification applications. Firstly, different with [15], this model is used to classify classical image data, not quantum data. Image data need to be encoded into quantum states to be processed by quantum hardware. We employ the qubit-efficient amplitude encoding method and an approximate preparation circuit, which has the potential to decrease the resource overhead on

This work is supported by National Natural Science Foundation of China (No. 61903016, No. 61803132) and by Alexander von Humboldt Fellowship, Germany.

this primary stage. Secondly, the original quantum circuits in [15] were specifically designed to process the phases of quantum states, which can not be directly used in our case even if a quantum encoder has been designed. In this paper, we use more expressive universal quantum gates to construct the quantum convolutional layers and pooling layers based on the amplitude encoding, which makes the QCNN model suitable to deal with grid type data like images. Thirdly, the training procedure of this model is based on the parameter-shift rule [20, 21], which can efficiently calculate the analytical gradients of loss functions on quantum circuits and get a faster yet more stable convergence rate, compared with various finite-difference based optimization algorithms.

To sum up, the major contributions of our work are as follows:

- We propose a new quantum convolutional neural network model for image classification applications with efficient quantum state encoding and preparation methods.
- We design special quantum circuits with more expressive universal quantum gates that are suitable to process image-encoded quantum states.
- We design the training algorithm of our model using the parameter-shift rule.

2 Preliminaries

Quantum computation is based on quantum mechanics and is fundamentally different from the classical computation based on binary circuits. It has several important properties, such as superposition, entanglement, and unitary transformation, thus showing powerful computing capability. Here we would like to introduce basic concepts of quantum computation.

2.1 Qubits

The *qubit* is the basic unit of information storage and operation in quantum computation, analog to a binary bit in classical computation. A qubit has two basic states represented by $|0\rangle$ and $|1\rangle$, respectively, corresponding to the ground state and excited state of a two-level quantum system. However, unlike the classical bit that can only take one value at any time, a qubit can be in any *superposition* state of $|0\rangle$ and $|1\rangle$:

$$|\psi\rangle = \alpha|0\rangle + \beta|1\rangle, \tag{1}$$

where $\alpha, \beta \in \mathbb{C}$ represent probability amplitudes and satisfy $|\alpha|^2 + |\beta|^2 = 1$. Choose $\{|0\rangle, |1\rangle\}$ as a basis, then any single qubit state $|\psi\rangle$ can be represented by a complex vector:

$$|\psi\rangle = \begin{bmatrix}\alpha\\ \beta\end{bmatrix} \in \mathbb{C}^2. \tag{2}$$

In quantum mechanics, we call a quantum system that has no interaction with the environment a *closed* quantum system. For n closed qubits, whose quantum states are respectively denoted as $|\psi^1\rangle, \cdots, |\psi^n\rangle$, the quantum state of the composite system composed of these n qubits is $|\Psi\rangle = |\psi^1\rangle \otimes \cdots \otimes |\psi^n\rangle$, which is general written as $|\psi^1 \cdots \psi^n\rangle$ for convenience. The linear space of an arbitrary n-qubit quantum state $|\Psi\rangle$ has a basis: $\{|00\cdots0\rangle, |00\cdots1\rangle, |11\cdots1\rangle\}$. Any quantum state $|\Psi\rangle$ in this linear space can be expressed as the following superposition state:

$$|\Psi\rangle = \sum_{i=0}^{2^n-1} \alpha_i|i\rangle, \alpha_i \in \mathbb{C}, \tag{3}$$

where $|i\rangle$ corresponds to the quantum state that can be described by the binary form of i, for example, $|7\rangle = |111\rangle$. If there is *entanglement* between qubits, the state of the composite quantum system can not be written as the tensor product of each single qubit states, such as the Bell state: $|\phi^+\rangle = \frac{|00\rangle + |11\rangle}{\sqrt{2}}$.

2.2 Quantum Gates

In quantum computation, the states of qubits can be manipulated by quantum gates. According to quantum mechanics, the evolution of a closed system is described by a *unitary transformation* U, satisfying $UU^\dagger = I$. For a quantum system with the initial state $|\psi_0\rangle = \sum_{i=0}^{2^n-1} \alpha_i|i\rangle$, a quantum gate performing a unitary transformation U behaves like the matrix-vector multiplication:

$$U|\psi_0\rangle = U\sum_{i=0}^{2^n-1} \alpha_i|i\rangle = \sum_{i=0}^{2^n-1} \beta_i|i\rangle. \tag{4}$$

Ref. [22] proved that any unitary transformation can be expressed as a finite sequence of gates from a set of basic quantum gates. In this work, the commonly used basic gates include single-qubit rotation gates, such as $RX(\theta), RY(\theta), RZ(\theta)$, and the controlled NOT gate $CNOT$. For example, the matrices and notations of several quantum gates are shown in Table.1.

Table 1: Matrices and notations of quantum gates

Gates	Matrices	Notations
RX	$\begin{bmatrix} cos(\frac{\theta}{2}) & -isin(\frac{\theta}{2}) \\ -isin(\frac{\theta}{2}) & cos(\frac{\theta}{2}) \end{bmatrix}$	$\|\psi_i\rangle$ — RX — $\|\psi_o\rangle$
$CNOT$	$\begin{bmatrix} 1 & 0 & 0 & 0 \\ 0 & 1 & 0 & 0 \\ 0 & 0 & 0 & 1 \\ 0 & 0 & 1 & 0 \end{bmatrix}$	$\|\psi_i\rangle$ — ● — $\|\psi_o\rangle$ X

2.3 Quantum Measurement

Information in the quantum system is not directly accessible and we need to perform the quantum *measurement* to obtain the information. For example, performing a projective measurement with Z *observable* on the qubit with state $|\phi\rangle = \alpha|0\rangle + \beta|1\rangle$ generates 1 and -1 with probability $p(1) = |\alpha|^2$ and $p(-1) = |\beta|^2$, respectively. Meanwhile, after the measurement, the quantum state intermediately changes to $|0\rangle$ or $|1\rangle$ state. Measurement results are stochastic, and one measurement can only get one possible value with the corresponding probability. Thus, we need to perform repeated measurements to get as accurate information about the state as possible. The expectation value of a specific measurement observable Z on state $|\phi\rangle$ can be expressed as:

$$\langle Z\rangle_{|\phi\rangle} \equiv \langle\phi|Z|\phi\rangle = |\alpha|^2 - |\beta|^2, \tag{5}$$

where $Z \equiv \begin{bmatrix}1 & 0\\ 0 & -1\end{bmatrix}$, $\langle\phi| = (|\phi\rangle)^\dagger$, and $\langle Z\rangle \in [-1, 1]$.

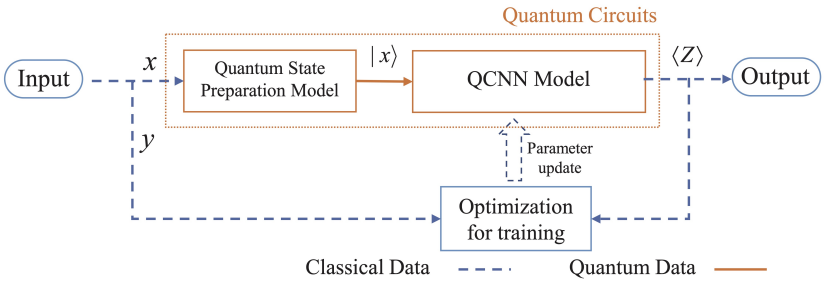

Fig. 1: Supervised learning framework of the proposed quantum convolutional neural network (QCNN). Dashed lines represent classical data and solid lines represent quantum data. The quantum circuits are marked with orange dotted box.

3 Quantum Convolutional Neural Network

Similar to the basic structure of classical neural networks, the supervised learning framework of the proposed QCNN is shown in Fig. 1. This is a quantum-classical hybrid framework, where the classical computer and quantum computer cooperate to complete the whole forward and training process of the QCNN. Three main sub-models are quantum state preparation model, QCNN model and Optimization model, of which the first two are quantum and the last is classical. In fact, this quantum-classical hybrid framework is widely used in recent quantum machine learning works [17, 23, 24]. In the near term, NISQ computers only have limited qubits and low circuit depths. By putting complex training calculations on classical computers, this hybrid framework helps explore the potential computational power of NISQ computers.

The overall framework of QCNN can be as follows. The quantum state preparation model first receives a classical image $\boldsymbol{x}$ and encodes the image grid data into a quantum state $|\boldsymbol{x}\rangle$. The QCNN model consisting of a sequence of quantum circuits then transforms and extracts the features in quantum states. At the end of the QCNN model, the quantum measurement block outputs expectation values $\langle Z\rangle$ as the classification results. The optimization model running on a classical computer updates the parameters of the QCNN model according to the differences between the true labels and the classification results.

3.1 Quantum State Preparation Model

State preparation is an essential block when using quantum machine learning algorithms to process classical data. There are two different encoding methods, including the basis encoding method and the amplitude encoding method. The basis encoding method treats two basic states of a qubit, $|0\rangle$ and $|1\rangle$, as binary values of a classical bit, 0 and 1. A n-qubit quantum system can then represent an integer or a floating-point number with a certain precision, for example $9 \rightarrow |1001\rangle$ [25]. The amplitude encoding method uses the probability amplitudes of a quantum state to store numbers. A n-qubit quantum system has 2^n amplitudes and can store 2^n imaginary numbers in principle. For a 2^n-dimensional real vector $\boldsymbol{x} = (x_0, x_1, \cdots, x_{2^n-1})^T$, the corresponding quantum state is $|\boldsymbol{x}\rangle = \sum_0^{2^n-1} x_i|i\rangle$. Obviously, the amplitude encoding method is more qubit-efficient than the basis encoding method and is widely used in many recent QML algorithms [26–28]. In this paper, the amplitude encoding method is used.

Despite being qubit-efficient, the preparation of amplitude encoding states requires much time and the quantum circuit resources. It has been shown that accurately preparing a n-qubit amplitude encoding state needs $O(2^n)$ time and quantum circuits with $O(2^n)$ depth [29, 30], which might eliminate the quantum advantages. Following the idea of [23], we build a state preparation model that can be trained to approximately encode an arbitrary vector. It consists of a simulation training circuit and a reconstruction circuit as shown in Fig. 2. The main idea is to train the simulation circuit to do the desired transformation and use the optimal parameters to prepare quantum states on the reconstruction circuit. The quantum gate $R(\theta^i)$ in Fig. 2 has 3 parameters and can be adjusted to achieve any single-qubit unitary transformation. With several layers of quantum gates stacked, the circuit has strong approximation capabilities.

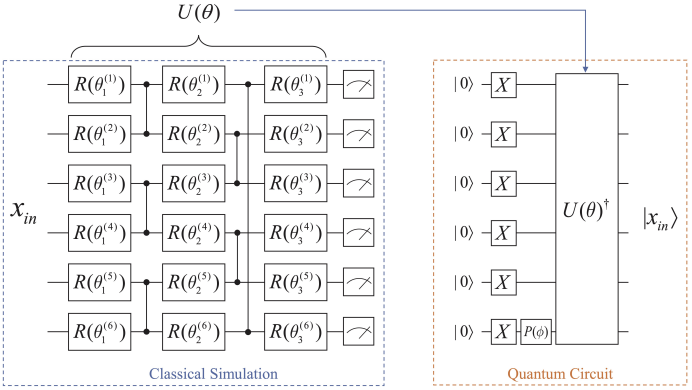

Fig. 2: State preparation model. The left figure is the simulation training circuit and the right figure is the reverse reconstruction circuit.

In the first step, we need to train the simulation circuit to transform the initial state $|\boldsymbol{x}_{in}\rangle$ to $|1\rangle^{\otimes n}$. It should be noted that this process runs in classical simulation, and for a given state $|\boldsymbol{x}_{in}\rangle$ it yields a specific set of gate parameters $\boldsymbol{\theta}$. The loss function is defined as:

$$f(\boldsymbol{\theta}) = \frac{1}{n}\sum_{i=1}^{n}\langle Z_i\rangle_{U(\boldsymbol{\theta})|\boldsymbol{x}_{in}\rangle}, \tag{6}$$

where $\langle Z_i\rangle$ is the expectation of Z measurement on the i-th qubit. Thus the training procedure iteratively evaluate the loss function and adjust parameters using gradient descent algorithm to minimize formula (6). Suppose that the loss function can be minimized to -1, then all measurement expectation values are -1, and thus the final quantum state of the circuit

before measurements is $e^{i\phi}|1\rangle^{\otimes n}$. It means that the circuit actually perform the transformation: $U(\boldsymbol{\theta}^*)|\boldsymbol{x}_{in}\rangle = e^{i\phi}|1\rangle^{\otimes n}$. The global phase term $e^{i\phi}$ is accessible in numerical simulation. In the second step, we use the parameters $\boldsymbol{\theta}^*$ to construct a reverse circuit on real quantum computers, where $P(\phi)$ represents the phase gate. The reverse circuit applies the transformation $U'(\theta) = U(\boldsymbol{\theta}^*)^\dagger \cdot (I^{\otimes n-1} \otimes P(\phi)) \cdot X^{\otimes n}$ on initial state $|0\rangle$, and outputs the desired quantum state $|\boldsymbol{x}_{in}\rangle$.

Since low depth circuits have limited approximation power, the loss function usually does not approach -1 close enough. In that case, the reconstructed state would differ from the desired state $|\boldsymbol{x}_{in}\rangle$ at a distance, so this model can only approximately prepare quantum states. However, this method has the advantage of systematic design and off-line training, which is still favorable in preparation of the quantum data.

3.2 QCNN Model

Analogous to classical CNNs, the QCNN model consists of quantum convolutional layers, quantum pooling layers, and a quantum fully connected (FC) layer, forming a hierarchical structure as shown in Fig. 3. The QCNN model's goal is to learn proper parameters so that encoded quantum states can be correctly mapped to their corresponding labels. The input of QCNN model is an image-encoded quantum state $|\boldsymbol{x}_{in}\rangle$. Parameterized quantum circuits apply transformations to extract features layer by layer. At the end of the QCNN model, quantum measurements are performed on specific qubits to get expectation values that indicate classification results.

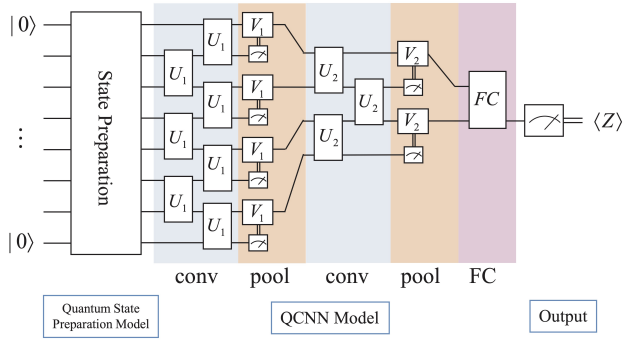

Fig. 3: Quantum circuits of QCNN, including the quantum state preparation model and the QCNN model.

3.2.1 Quantum convolutional layer

A quantum convolutional layer comprises two-qubit unitary operations U_i, where i indicates the i-th convolutional layer. Two features of convolutional layers in classical CNNs are local connectivity and parameter sharing. In the quantum convolutional layer, two-qubit unitary operations are applied to neighboring qubits and have only local effects, reflecting the local connectivity feature. Besides, in one quantum convolutional layer, all applied unitary operations have the same parameters, reflecting the parameter sharing feature. Since image information is encoded in amplitudes of quantum states, It is important to use expressive unitary operations that can achieve a big range of transformations on the amplitudes. The most expressive two-qubit unitary operation is the *universal* quantum circuit that can achieve arbitrary transformations $U \in \mathcal{SU}(4)$. Some works offer different decomposition of a universal two-qubit quantum gate based on different basic quantum gate sets [31, 32]. In this work, we apply the decomposition method of [31] as shown in Fig. 4 that requires only gates from $\{CNOT, RY, RZ\}$, where the quantum gates $a, b, c, d \in \mathcal{SU}(2)$ are universal single-qubit gates that can be decomposed into $RZ \cdot RY \cdot RZ$ [33]. The universal gate U_i has 15 adjustable parameters, which is exactly the degree of freedom of $\mathcal{SU}(4)$.

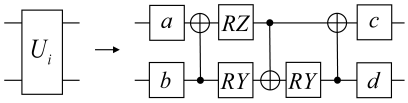

Fig. 4: Decomposition of a universal two-qubit unitary gate used in quantum convolutional layers.

3.2.2 Quantum pooling layer

In a quantum pooling layer, a portion of qubits are measured and their outcomes determine whether applying single-qubit gates V_i on their neighbor qubits. With quantum measurements and classically controlled gates, quantum pooling layers reduce the dimension of the feature mapping as well as introduce nonlinearities. To get better approximation power, the gate is supposed to have arbitrary control state and can apply arbitrary single qubit transformations. Specifically, the proposed quantum circuit is depicted in Fig. 5, where $a, b \in \mathcal{SU}(2)$ are universal single-qubit gates. In terms of the principle of deferred measurement [33], measurements commute with quantum gates when the qubit being measured is a control qubit, thus the right side circuit has exactly the same properties as the left side one.

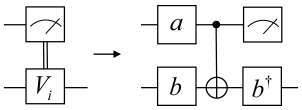

Fig. 5: Quantum circuits for quantum pooling layers.

3.2.3 Quantum FC layer

After applying several layers of quantum convolutional layers and pooling layers, the number of qubits will decrease. When the system size is relatively small, a quantum FC layer is applied on the remaining qubits to perform classification on the extracted features. We employ the strongly entangling circuits proposed in [34] as the FC layer, which consists of universal single-qubit quantum gates and $CNOT$ gates.

At the end of the QCNN model, measurements are performed on a fixed number of output qubits to get expectation values. Formally, the output of the QCNN model for input $\boldsymbol{x}_{in}$ is denoted as $f(\boldsymbol{\theta}, \boldsymbol{x}_{in})$. There are various ways to map expectation values to classification results. For binary classification tasks, it is convenient to measure one qubit and consider the expectation value as the output: $f(\boldsymbol{\theta}, \boldsymbol{x}_{in}) \equiv \langle Z \rangle$. Then $\langle Z \rangle \geq 0$ indicates classifying the sample to one class and $\langle Z \rangle < 0$ indicates classifying the sample to the other class.

3.3 Optimization of QCNN

Similar to gradient-based optimization algorithms for classical CNNs, we proposed a stochastic gradient descent (SGD)

algorithm for optimizing the proposed QCNN model. Like weights in classical CNNs, the parameters of quantum gates that compose the QCNN model are to be optimized. The SGD for QCNN aims at adjusting parameters in terms of gradients of the loss function to learn proper mappings. To achieve the optimization, gradients of the loss function with respect to quantum gate parameters are required, and then a quantum SGD scheme can be applied.

3.3.1 Calculation of the gradients of quantum circuits

Analytical gradients of quantum circuits can be calculated using the chain rule and the parameter-shift rule [20, 21]. Assume that the loss function $\ell_{\boldsymbol{\theta}}$ is a function of the expectation values$\{\langle O_k\rangle_{\boldsymbol{\theta}}\}_{k=1}^{K}$, then by the chain rule, the partial derivative $\frac{\partial \ell_{\boldsymbol{\theta}}}{\partial \theta_j}$ can be expressed as a function of these expectation values as well as their derivatives $\frac{\partial \langle O_k\rangle_{\boldsymbol{\theta}}}{\partial \theta_j}$. According to the parameter-shift rule, for qubit-based quantum computing, the derivatives of quantum expectation values can be expressed as the combination of expectation values of similar quantum circuits:

$$\frac{\partial \langle O_k\rangle_{\boldsymbol{\theta}}}{\partial \theta_j} = \frac{\langle O_k\rangle_{\boldsymbol{\theta}+\frac{\pi}{2}\boldsymbol{e}_j} - \langle O_k\rangle_{\boldsymbol{\theta}-\frac{\pi}{2}\boldsymbol{e}_j}}{2}. \tag{7}$$

The expectation value $\langle O_k\rangle_{\boldsymbol{\theta}\pm\frac{\pi}{2}\boldsymbol{e}_j}$ indicates that change the i-th parameter of the origin circuit by $\frac{\pi}{2}$ and get the corresponding expectation value. This calculation method is accurate and is easily implementable on NISQ computers.

3.3.2 SGD optimization

With gradients accessible, we can construct the SGD optimization algorithm. For each iteration, a subset of training dataset is selected to evaluate the loss function, and then parameters are updated with respect to learning rates and gradients. Pseudocode of SGD is shown in Algorithm 1.

Algorithm 1 SGD Optimization for QCNN

Require: Quantum states $\{|\boldsymbol{x}_i\rangle^{train}\}_{i=1}^{S}$ for the dataset $\{\boldsymbol{x}_i^{train}, y_i\}_{i=1}^{S}$, the QCNN model with parameters $\boldsymbol{\theta}$, the loss function $\ell_{\boldsymbol{\theta}} : |\boldsymbol{x}_i\rangle \to \mathbb{R}$, the iteration time T, the batch size s, and the learning rate $\{\eta(t)_{t=0}^{T-1}\}$.
Ensure: The optimized parameters $\boldsymbol{\theta}^*$.
1: Randomly initialize the parameters $\boldsymbol{\theta}^*$ in the range of $[0, 2\pi]$.
2: **for** $t \in \{0, 1, \cdots, T-1\}$ **do**
3: Randomly select a set of samples with index $i \in I_t$ with size s.
4: Calculate the gradient $\nabla_{\boldsymbol{\theta}}\ell_{I_t}(\boldsymbol{\theta})|_{\boldsymbol{\theta}=\boldsymbol{\theta}^{(t)}}$ in terms of the parameter-shift rule.
5: Update parameters $\boldsymbol{\theta}^{(t+1)} = \boldsymbol{\theta}^{(t)} - \eta(t)\cdot\nabla_{\boldsymbol{\theta}}\ell_{I_t}(\boldsymbol{\theta})|_{\boldsymbol{\theta}=\boldsymbol{\theta}^{(t)}}$.
6: **end for**
7: Output optimized parameters $\boldsymbol{\theta}^* = \boldsymbol{\theta}^{(T)}$

4 Experiments

In this section, the image dataset MNIST [2] is employed to evaluate the performance of the proposed QCNN on image classification tasks. For simplicity, we construct a binary classification task that is to classify only two classes of samples in the dataset. Numerical simulations of the experiments are performed with Pennylane Python Package [35].

4.1 Dataset

The MNIST dataset includes images of handwritten digits and corresponding labels of the ten digits from 0 to 9, of which the training set has 60000 samples and 10000 test samples. Each image is gray-scale and has a size of 28×28. For numerical simulation, these images are down-sampled into 8×8 to fit the QCNN model with 6 qubits. Since the numbers of samples that belong to each digit are different, we randomly select 5000 samples labeled as 3's and 6's respectively from the training set to build a balanced training dataset, and similarly build a test dataset with 1700 samples. Besides, all down-sampled data are normalized to fit the amplitude encoding. The label of digit 3 is set to 1 and -1 for digit 6.

Formally, let $D^{train} = \{\boldsymbol{x}_i^{train}, y_i^{train}\}_{i=1}^{S}$ be the training dataset and $D^{test} = \{\boldsymbol{x}_i^{test}, y_i^{test}\}_{i=1}^{Q}$ be the test dataset, where $\boldsymbol{x}_i \in \mathbb{R}^N, y_i \in \{-1, 1\}, S = 10000, Q = 1700, N = 64$.

4.2 Training and Prediction

We employ the SGD optimization shown in Algorithm 1 to train the QCNN model in Section 3.2. For the binary classification task, the model output $f(\boldsymbol{\theta}, \boldsymbol{x}_i)$ is define as a quantum measurement expectation value on a specific qubit. Note that $f(\boldsymbol{\theta}, \boldsymbol{x}_i) \in [-1, 1]$ due to properties of the quantum measurement. The loss function $\ell_{\boldsymbol{\theta}}$ is defined as:

$$\ell_{I_t}(\boldsymbol{\theta})|_{\boldsymbol{\theta}} = \frac{1}{s}\sum_{i=1}^{s}(f(\boldsymbol{\theta}, \boldsymbol{x}_i^{train}) - y_i^{train})^2. \tag{8}$$

For predication, the classification result $\hat{f}(\boldsymbol{\theta}, \boldsymbol{x}_i)$ is defined as:

$$\hat{f}(\boldsymbol{\theta}, \boldsymbol{x}_i) = \begin{cases} 1, & \text{if } f(\boldsymbol{\theta}, \boldsymbol{x}_i) \geq 0 \\ -1, & \text{if } f(\boldsymbol{\theta}, \boldsymbol{x}_i) < 0 \end{cases}, \tag{9}$$

and the test accuracy acc is defined as:

$$acc = \frac{1}{Q}\sum_{i=1}^{Q} I(\hat{f}(\boldsymbol{\theta}, \boldsymbol{x}_i^{test}) = y_i^{test}), \tag{10}$$

where $I(\cdot)$ is the indicator function.

4.3 Experimental Results and Comparisons

The experimented QCNN model has 6 qubits and is composed of 2 quantum convolutional layers, 2 quantum pooling layers, and 1 quantum FC layer. The number of trainable parameters is 54. The number of the training iteration $T = 1000$, the batch size $s = 16$ and the decayed learning rate is adopted as $\{0.1, 0.075, 0.05, 0.025\}$. The test accuracy acc is evaluated on the whole test dataset.

The loss function curve and the test accuracy curve during the training iteration are shown in Fig. 6 and Fig. 7. It can be seen that the loss value had a clear downward trend and reached an average value of around 0.45 finally. The test accuracy improved quickly in the first 50 iterations and then gradually reached the highest value of 96.65%.

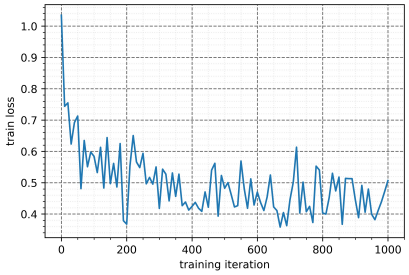

Fig. 6: The training loss of QCNN during the training iteration.

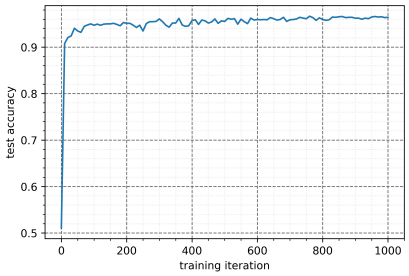

Fig. 7: The test accuracy of QCNN during the training iteration.

As discussed above, the proposed QCNN could accurately yet efficiently classify the MNIST dataset. Compared with the QNN model in [17], which requires more than $2n$ qubits to classify images with a size of 2^n, the proposed QCNN only requires n qubits and is more qubit-efficient.

5 Conclusions

In this paper, a novel quantum convolutional neural network model, namely QCNN, for image classification applications has been presented. It is built on parameterized quantum circuits and has a similar hierarchical structure as classical CNNs. The amplitude encoding method and an approximate quantum state preparation model have been employed to keep qubit-efficient as well as low state preparation overhead. Structures of the three kinds of quantum layers imitate the characteristics of classical CNNs, and the specially designed quantum gates provide unique expressive power. Besides, the classification performance has been numerical evaluated on the MNIST dataset. This work has primarily explored the classification capability of QCNN, and other properties, such as optimization rate, convergence guarantee, and quantum advantages, are worth further exploring.

References

[1] Y. LeCun, B. E. Boser, J. S. Denker, D. Henderson, R. E. Howard, W. E. Hubbard, *et al.*, Handwritten digit recognition with a back-propagation network, in *Advances in neural information processing systems*, 1990: 396-404.

[2] Y. LeCun, L. Bottou, Y. Bengio, and P. Haffner, Gradient-based learning applied to document recognition, *Proceedings of the IEEE*, 86(11): 2278–2324, 1998.

[3] W. Rawat and Z. Wang, Deep convolutional neural networks for image classification: A comprehensive review, *Neural computation*, 29(9): 2352-2449, 2017.

[4] S. Lu, Y. Zheng, X. Wang, and R. Wu, Quantum machine learning (in Chinese), *Control Theory & Applications*, 34(11): 1429-1436, 2017.

[5] M. Benedetti, E. Lloyd, S. Sack, and M. Fiorentini, Parameterized quantum circuits as machine learning models, *Quantum Science and Technology*, 4(4): 043001, 2019.

[6] J. Biamonte, P. Wittek, M. Pancotti, P. Rebentrost, N. Wiebe, and S. Lloyd, Quantum machine learning, *Nature*, 549(7671): 195-202, 2017.

[7] S. Wu, S. Jin, D. Wen, and X. Wang, Quantum reinforcement learning in continuous action space, *arXiv preprint*, arXiv:2012.10711, 2020.

[8] R. Wu, X. Cao, P. Xie, and Y. Liu, End-to-end quantum machine learning implemented with controlled quantum dynamics, *Physical Review Applied*, 14(6): 064020, 2020.

[9] F. Arute, K. Arya, R. Babbush, D. Bacon, J. C. Bardin, R. Barends, *et al.*, Quantum supremacy using a programmable superconducting processor, *Nature*, 574(7779): 505-510, 2019.

[10] M. Mohseni, P. Read, H. Neven, S. Boixo, V. Denchev, R. Babbush, *et al.*, Commercialize quantum technologies in five years, *Nature*, 543(7644): 171-174, 2017.

[11] J. Preskill, Quantum computing in the NISQ era and beyond, *Quantum*, 2: 79-98, 2018.

[12] S. C. Kak, Quantum neural computing, *Advances in imaging and electron physics*, 94: 259-313, 1995.

[13] M. Schuld, I. Sinayskiy, and F. Petruccione, The quest for a Quantum Neural Network, *Quantum Information Processing*, 13(11): 2567–2586, 2014.

[14] Y. Lü, Q. Gao, J. Lü, Y. Pan, and D. Dong, Recent advances of quantum neural networks on the near term quantum processor (in Chinese), *Scientia Sinica Technologica*, doi: 10.1360/SST-2020-0459, accepted.

[15] I. Cong, S. Choi, and M. D. Lukin, Quantum convolutional neural networks, *Nature Physics*, 15(12): 1273–1278, 2019.

[16] M. Henderson, S. Shakya, S. Pradhan, and T. Cook, Quanvolutional neural networks: Powering image recognition with quantum circuits, *Quantum Machine Intelligence*, 2(1): 1-9, 2020.

[17] Y. Li, R. Zhou, R. Xu, J. Luo, and W. Hu, A quantum deep convolutional neural network for image recognition, *Quantum Science and Technology*, 5(4): 044003, 2020.

[18] Y. Du, M. H. Hsieh, T. Liu, and D. Tao, Expressive power of parametrized quantum circuits, *Physical Review Research*, 2(3): 033125, 2020.

[19] S. Bravyi, D. Gosset, and R. König, Quantum advantage with shallow circuits, *Science*, 362(6412): 308–311, 2018.

[20] K. Mitarai, M. Negoro, M. Kitagaw, and K. Fujii, Quantum circuit learning, *Physical Review A*, 98(3): 032309, 2018.

[21] M. Schuld, V. Bergholm, C. Gogolin, J. Izaac, and N. Killoran, Evaluating analytic gradients on quantum hardware, *Physical Review A*, 99(3): 032331, 2019.

[22] D. E. Deutsch, Quantum computational networks, *Proceedings of the Royal Society of London. A. Mathematical and Physical Sciences*, 425(1868): 73-90, 1989.

[23] K. Zhang, M. H. Hsieh, L. Liu, and D. Tao, Toward trainability of quantum neural networks, *arXiv preprint*, arXiv:2011.06258, 2020.

[24] J. R. McClean, J. Romero, B. Ryan, and A. Aspuru-Guzik, The theory of variational hybrid quantum-classical algorithms, *New Journal of Physics*, 18(2): 023023, 2016.

[25] M. Schuld, I. Sinayskiy, and F. Petruccione, Simulating a perceptron on a quantum computer, *Physics Letters A*, 379(7): 660-663, 2015.

[26] A. W. Harrow, A. Hassidim, and S. Lloyd, Quantum algorithm for linear systems of equations, *Physical Review Letters*, 103(15):

150502, 2009.

[27] P. Rebentrost, M. Mohseni, and S. Lloyd, Quantum support vector machine for big data classification, *Physical Review Letters*, 113(13): 130503, 2014.

[28] S. Yan, H. Qi, and W. Cui, Nonlinear quantum neuron: A fundamental building block for quantum neural networks, *Physical Review A*, 102(5): 052421, 2020.

[29] M. Schuld, *Supervised learning with quantum computers*. Cham: Springer, 2018, 139-151.

[30] D. K. Park, F. Petruccione, and J. K. K. Rhee, Circuit-based quantum random access memory for classical data, *Scientific Reports*, 9: 3949, 2019.

[31] V. V. Shende, I. L.Markov, and S. S. Bullock, Minimal universal two-qubit controlled-NOT-based circuits, *Physical Review A*, 69(6): 062321, 2004.

[32] R. R. Tucci, An introduction to Cartan's KAK decomposition for QC programmers, *arXiv preprint*, quant-ph/0507171, 2005.

[33] M. A. Nielsen and I. L. Chung, *Quantum Computing and Quantum Information*. New York: Cambridge University Press, 2000, 61-73.

[34] M. Schuld, A. Bocharov, K. M. Svore, and N. Wiebe, Circuit-centric quantum classifiers, *Physical Review A*, 101(3): 032308, 2020.

[35] V. Bergholm, J. Izaac, M. Schuld, C. Gogolin, M. S. Alam, S. Ahmed, *et al.*, Pennylane: Automatic differentiation of hybrid quantum-classical computations, *arXiv preprint*, arXiv:1811.04968, 2018.